Nonlinear low-frequency structures in the auroral plasma in the presence of an oxygen beam including charge separation

S. Moolla,[1] R. Bharuthram,[2] S. V. Singh,[3,a)] G. S. Lakhina,[3] and R. V. Reddy[3]
[1]*University of KwaZulu-Natal, Durban 4000, South Africa*
[2]*University of the Western Cape, Modderdam Road, Belville 7535, South Africa*
[3]*Indian Institute of Geomagnetism, New Panvel (W), Navi Mumbai 410218, India*

(Received 7 August 2009; accepted 5 January 2010; published online 11 February 2010)

Observations from the Fast Auroral SnapshoT (FAST) satellite indicate that the parallel and perpendicular (to the Earth's magnetic field) electric field structures exhibit a spiky appearance. In this study, a magnetized plasma system consisting of protons, electrons, and a cold oxygen ion beam is considered. Both background electrons and protons are treated as hot species with Boltzmann density distributions. The dynamics of the oxygen ion beam is governed by the fluid equations. Effect of charge separation is studied on nonlinear fluctuations arising from a coupling of ion cyclotron and ion-acoustic waves. A scan of parameter space reveals a range of solutions for the parallel electric field from sinusoidal to sawtooth to highly spiky waveforms. The inclusion of charge separation effects tends to in most cases increase the frequency of oscillation of the nonlinear structures. In the case of a weakly magnetized plasma, the amplitude of the oscillations are found to be constant while they are modulated for a strongly magnetized plasma. The findings are compared with satellite observations. © *2010 American Institute of Physics*.
[doi:10.1063/1.3299328]

I. INTRODUCTION

Satellite observations over the last three decades have indicated the presence of broadband electrostatic noise (BEN) in different regions of the Earth's magnetosphere, e.g., along auroral field lines,[1] polar cusp region,[2] magnetosheath,[3] and plasma sheet boundary layer,[4] etc. High-time resolution waveform measurements by several spacecrafts[3–6] have shown that these BENs consist of nonlinear structures, i.e., electrostatic solitary waves (ESWs). These ESWs are isolated pulses observed in the parallel electric field and are usually bipolar or tripolar. They have been observed in plasma sheet boundary layer,[4] bow shock,[7] magnetosheath,[3] polar cap boundary layer,[8,9] and in the auroral acceleration region.[6,10] Their amplitudes can vary from typically a few mV/m in the plasma sheet boundary layer to 200 mV/m or higher at polar altitudes.[11] The ESWs are generally observed in association with electron or/and ion beams. Usually, in the auroral zone, the ESWs associated with the ion beams have negative potentials and propagate at velocities of the order of ion-acoustic (IA) or beam speed[12–14] and have been interpreted in terms of ion solitary waves or solitons.[14,15] Several theoretical studies have been undertaken to study nonlinear IA waves in multispecies plasmas.[15–23]

The electrostatic ion cyclotron (EIC) waves are found to be unstable to current-driven instabilities in the auroral region[24] and play important role in heating and acceleration of the plasma.[25] The EIC waves have been frequently observed by several satellites, e.g., S3–3,[26] Viking,[27] Polar,[5] and FAST[6,28] in the auroral region of the Earth's magnetosphere. Polar satellite observations[5] have shown that the parallel as well as perpendicular electric field exhibits spiky structures. FAST observations in the upward current region showed large amplitude spiky structures associated with parallel electric fields[6] whereas in the downward current region spiky electric field structures were shown to exhibit in both perpendicular and parallel components. The perpendicular electric field structures represented ion cyclotron waves at a frequency $f \sim 200$ Hz. On the other hand, the parallel electric field showed a spiky waveform at a lower frequency. Large amplitude electrostatic waves near the cyclotron frequencies of H^+, O^+, and He^+ have also been observed by FAST satellite during the nightside auroral zone crossing.[28] Satellite observations in the auroral acceleration region have shown presence of oxygen ion beams.[14,28] Nonlinear EIC instability driven by counter-streaming ion beams have been studied in equatorial outer plasmasphere.[29] It was found that when the beams are sufficiently fast, instability occurs through the coupling of the Doppler-shifted ion-cyclotron modes of the two beams. The dominant mode occurs when the modes corresponding to the fundamental cyclotron harmonic couple.

A linear coupling between EIC waves and IA waves near the second harmonic ion cyclotron frequency has been studied by Ohnuma *et al.*[30] Later on, the coupling between the two modes was also detected experimentally in an argon plasma.[31] Temerin *et al.*[32] studied the nonlinear EIC waves propagating nearly perpendicular to the magnetic field. They observed spiky structures in the perpendicular electric field for large Mach numbers and applied their results to explain the S3-3 satellite observations. Lee and Kan[33] studied the nonlinear coupling of the EIC and IA waves in a magnetized plasma. Using a "Sagdeev potential" approach, they investigated spiky and solitary wave structures along the direction

a)Electronic mail: satyavir@iigs.iigm.res.in.

of wave propagation, oblique to ambient magnetic field. Reddy *et al.*[34] studied nonlinear low-frequency electric field structures in a two-component magnetized plasma consisting of cold ions and warm electrons. It was shown that for sufficiently large values of the driver electric field, IA and ion cyclotron modes couple and generate sawtooth and highly spiky periodic waveforms. Results were found to be in good agreement of the satellite observations. Later on Bharuthram *et al.*[35] studied the effect of ion temperature on low-frequency nonlinear waves in the auroral plasma. It was found that the effect of finite ion temperature is to suppress the nonlinearity in the ion cyclotron waves and decreases the periodicity of the oscillations. However, the periodicity of the IA wave increases with increasing ion temperature. Ganguli *et al.*[36] studied the low-frequency oscillations in a plasma with spatially variable field-aligned flow. It was shown that a transverse velocity gradient in the parallel ion flow can generate multiple cyclotron harmonic waves, as predicted earlier by Lakhina[37] for the case of plasma sheet boundary layer region. Generation of spiky electric field structures associated with multiharmonic EIC waves was studied by Kim *et al.*[38] in a double ended Q machine. They observed that a linear combination of a multiharmonic spectrum of EIC waves could lead to the generation of spiky electric potential waveforms when the harmonics have comparable amplitudes and their phases are locked. Moolla *et al.*[39,40] examined high-frequency nonlinear waves in the Earth's magnetosphere using the approach of Reddy *et al.*[34] They considered a three component plasma model consisting of hot electrons, cold electrons, and cold ions. They found similar electric field structures, from sinusoidal to sawtooth to spiky waveforms through a coupling of electron-acoustic and the electron cyclotron modes. An important finding was that the periods of the spiky nonlinear structures varied with the hot electron drift speed. Consequently, they associated the rapid variation in the period of the spiky structures observed in satellite measurements to the electrons being accelerated in bursts. A relationship between pulse widths and periods of the ESWs was found to be in compliance of Geotail observations.[41]

Motivated by the FAST observations of waves near the oxygen cyclotron frequencies in the auroral region, Reddy *et al.*[42,43] studied nonlinear low-frequency electrostatic waves in a magnetized plasma consisting of protons, electrons, and oxygen ion beams. They showed that a range of periodic solutions varying from sinusoidal to sawtooth and highly spiky wave forms could be obtained depending on the plasma parameters considered. Their results were well within the range of FAST satellite observations.[28] Their analysis was based on the quasineutral approximation and could lead to a single nonlinear differential equation in the rest frame of the propagating wave. In this paper, we extend the work of Reddy *et al.*[43] by including the Poisson equation, thereby allowing for the charge separation effect and numerically solve the resulting set of coupled nonlinear equations. In this paper, we assume phase velocity to be greater than the ion beam thermal speed, hence, the assumption of a cold ion beam. However, one can extend the work by including the oxygen ion thermal effects. Our findings are then compared to satellite observations. The layout of this paper is as follows. In Sec. II, we present the basic theory and the numerical results are presented in Sec. III. Finally, our findings are summarized in Sec. IV.

II. BASIC THEORY

We consider a homogeneous magnetized three component, collisionless plasma consisting of a background species of protons, electrons, as well as a cold oxygen ion beam drifting along the magnetic field with speed v_0. The finite amplitude ion cyclotron and IA waves are propagating in the x direction at an angle θ to the magnetic field $\vec{B}_0$, which is assumed to be in the x-z plane and spatial variations are allowed only in the x direction. Here, phase velocity of the oscillations is considered to be smaller in comparison with the electron and proton thermal velocities. Thus, the Boltzmann distribution for the stationary hot electrons and protons are given, respectively, by

$$n_e = n_{e0} \exp(e\phi/T_e) \tag{1}$$

and

$$n_p = n_{p0} \exp(-e\phi/T_p), \tag{2}$$

where $n_{e0,p0}$ and $T_{e,p}$ are the ambient densities and temperatures of the electrons and protons, respectively.

The basic set of fluid equations for the beam of cold oxygen ions is given by

$$\frac{\partial n_i}{\partial t} + \frac{\partial n_i v_{ix}}{\partial x} = 0, \tag{3}$$

$$\frac{\partial v_{ix}}{\partial t} + v_{ix}\frac{\partial v_{ix}}{\partial x} = -\frac{e}{m_i}\frac{\partial \phi}{\partial x} + \Omega_i v_{iy} \sin\theta, \tag{4}$$

$$\frac{\partial v_{iy}}{\partial t} + v_{ix}\frac{\partial v_{iy}}{\partial x} = \Omega_i v_{iz} \cos\theta - \Omega_i v_{ix} \sin\theta, \tag{5}$$

$$\frac{\partial v_{iz}}{\partial t} + v_{ix}\frac{\partial v_{iz}}{\partial x} = -\Omega_i v_{iy} \cos\theta, \tag{6}$$

where n_i is the oxygen ion density v_{ix}, v_{iy} and v_{iz} are the components of the oxygen ion velocity along the x, y, and z directions, respectively, $\Omega_i = eB_0/m_i$ is the oxygen ion cyclotron frequency, m_i is the oxygen ion mass, and ϕ is the electrostatic potential of the waves. Our system is closed with the Poisson equation

$$\frac{\partial^2 \phi}{\partial x^2} = -\frac{e}{\epsilon_0}(n_i + n_p - n_e). \tag{7}$$

A. Linear Analysis

Before proceeding with the nonlinear analysis, we investigate the linear modes of the system. In this limit, Eqs. (1)–(6) give rise to the following dispersion relation:

$$\omega^2 = \tfrac{1}{2}(\Omega_i^2 + F^2) \pm \tfrac{1}{2}[(\Omega_i^2 + F^2)^2 - 4F^2\Omega_i^2 \cos^2\theta]^{1/2}, \tag{8}$$

where $F^2 = k^2C_{sf}^2/(1 + k^2C_{sf}^2/\omega_{pi}^2)$, where k is the wave number, $C_{sf} = [n_{i0}T_eT_p/m_i(n_{e0}T_p + n_{p0}T_e)]^{1/2}$ is the ef-

fective IA speed for a three component plasma, and $\omega_{pi}=(4\pi n_{i0}e^2/m_i)^{1/2}$ is the ion plasma frequency. By defining $R=\omega_{pi}/\Omega_i$, we can express F^2 (in a more convenient form) as $F^2=k^2C_{sf}^2/(1+k^2\rho_{i_{\rm eff}}^2/R^2)$ where $\rho_{i_{\rm eff}}=C_{sf}/\Omega_i$ is the effective ion Larmor radius. The solutions to this dispersion relation in the limit $(\Omega_i^2+F^2)^2 \gg 4F^2\Omega_i^2\cos^2\theta$ yields two modes, provided $R^2 \gg k^2\rho_{i_{\rm eff}}^2$. [In this limit, we recover Eq. (8) of Reddy *et al.*[43]] The higher frequency mode (ω_+) is given by

$$\omega_+ \approx \Omega_i(1+k^2\rho_{i_{\rm eff}}^2)^{1/2}, \tag{9}$$

which is the ion cyclotron mode. The lower frequency mode (ω_-), which is the IA mode, is given by:

$$\omega_- \approx \frac{kC_{sf}\cos\theta}{(1+k^2\rho_{i_{\rm eff}}^2)^{1/2}}. \tag{10}$$

It must be emphasized that space charge effects via Poisson equation allows modes with large wave numbers and this is reflected via the term $(1+k^2\rho_{i_{\rm eff}}^2)^{1/2}$ in our Eqs. (9) and (10) in the linear dispersion relations for the ion cyclotron and IA modes, respectively. However, the linear frequency of ion cyclotron (IA) mode increases (decreases) with wave number as shown by Eqs. (9) and (10), respectively. It is noted here that if one excludes the charge separation effects the term $(1+k^2\rho_{i_{\rm eff}}^2)^{1/2}$ will reduce to 1.

B. Nonlinear analysis

For the analysis, we transform to a stationary frame $s=(x-Vt)/(V/\Omega_i)$ and normalize v, t, x, and ϕ with respect to the oxygen IA speed $C_s=(T_e/m_i)^{1/2}$, Ω_i^{-1}, $\rho_i=C_s/\Omega_i$, and T_e/e, respectively.

In Eqs. (3)–(6), we replace $\partial/\partial t$ by $-\Omega_i(\partial/\partial s)$ and $\partial/\partial x$ by $(\Omega_i/V)(\partial/\partial s)$. In addition, we define $E=-\partial\psi/\partial s$ where $\psi=e\phi/T_e$. We use the following (initial) conditions: $\psi=0$, $\partial\psi/\partial s=-E_0$, $\partial^2\psi/\partial s^2=0$, $n_i=n_{i0}$, and $v_x=v_0\cos\theta$ at $s=0$. The evolution of plasma system is then determined by the following set of nonlinear, normalized first order differential equations:

$$\frac{\partial\psi}{\partial s}=-E, \tag{11}$$

$$\frac{\partial E}{\partial s}=R^2M^2(n_{in}+n_{pn}-n_{en}), \tag{12}$$

$$\frac{\partial n_{in}}{\partial s}=\frac{n_{in}^3[-E-Mv_{iyn}\sin\theta]}{(M-\delta\cos\theta)^2N_{i0}^2}, \tag{13}$$

$$\frac{\partial v_{iyn}}{\partial s}=(n_{in}(M-\delta\cos\theta)^{-1}/N_{i0}) \times\left[\left(M-\frac{(M-\delta\cos\theta)N_{i0}}{n_{in}}\right)\sin\theta-v_{izn}\cos\theta\right], \tag{14}$$

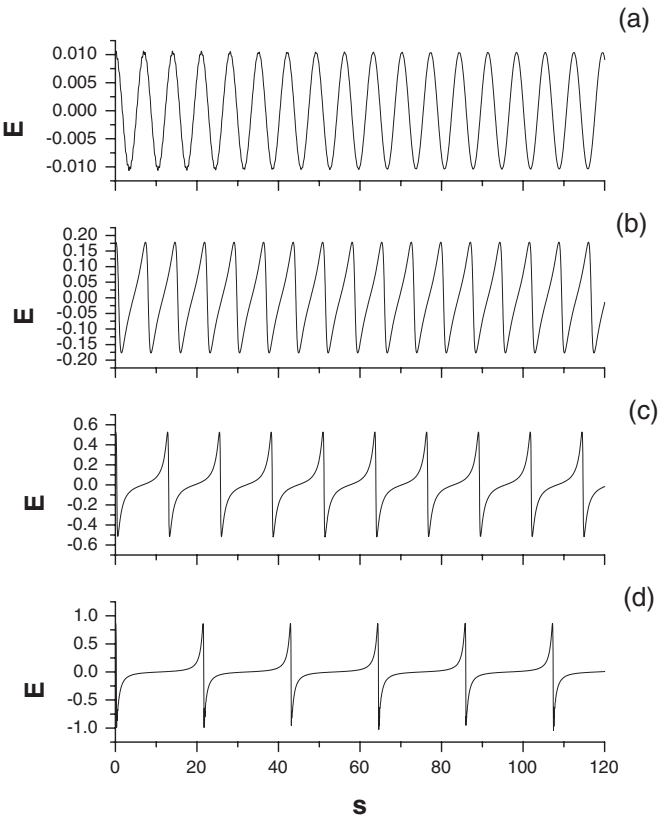

FIG. 1. Numerical solution of the normalized parallel electric field for the parameters $\theta=2°$, $M=1.25$, $N_{i0}=0.75$, $\delta=0.0$, $\alpha=0.1$, $R=10$, and $E_0=0.01$ (a), 0.175 (b), 0.50 (c), and 0.80 (d).

$$\frac{\partial v_{izn}}{\partial s}=n_{in}\frac{Mv_{iyn}\cos\theta}{(M-\delta\cos\theta)N_{i0}}. \tag{15}$$

In Eqs. (11)–(15), $M=V/C_s$ is the Mach number, $N_{i0}=n_{i0}/n_{e0}$ is the normalized equilibrium ion density, and $\delta=v_0/C_s$ is the normalized flow velocity of the oxygen ion beam at $s=0$. The normalized electron and proton density distributions are given by

$$n_{en}=\exp(\psi), \tag{16}$$

and

$$n_{pn}=N_{p0}\exp(-\alpha\psi), \tag{17}$$

where $N_{p0}=n_{p0}/n_{e0}$ is the normalized proton ambient density, $\alpha=T_e/T_p$ is the electron-proton temperature ratio, and $\psi=e\phi/T_e$ is the normalized potential The additional "n" subscript inserted indicates normalized quantities. It must be pointed out here that the two modes, i.e., ion cyclotron and IA modes nonlinearly couple through convective derivative terms in Eqs. (4)–(6).

III. NUMERICAL RESULTS

Equations (11)–(15) are solved using the Runge-Kutta technique[44] for plasma parameters encountered on the auroral field lines. The method involves providing initial values to plasma parameters and using the RK-4 subroutine to advance the functions with a suitable step length. The initial

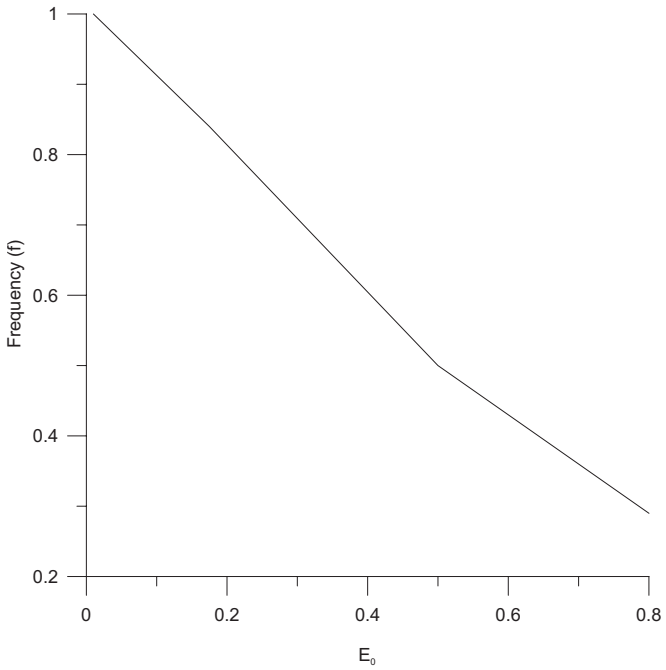

FIG. 2. Shows the variation in frequency (f) of the nonlinear structures with driver field (E_0) for the parameters of Fig. 1.

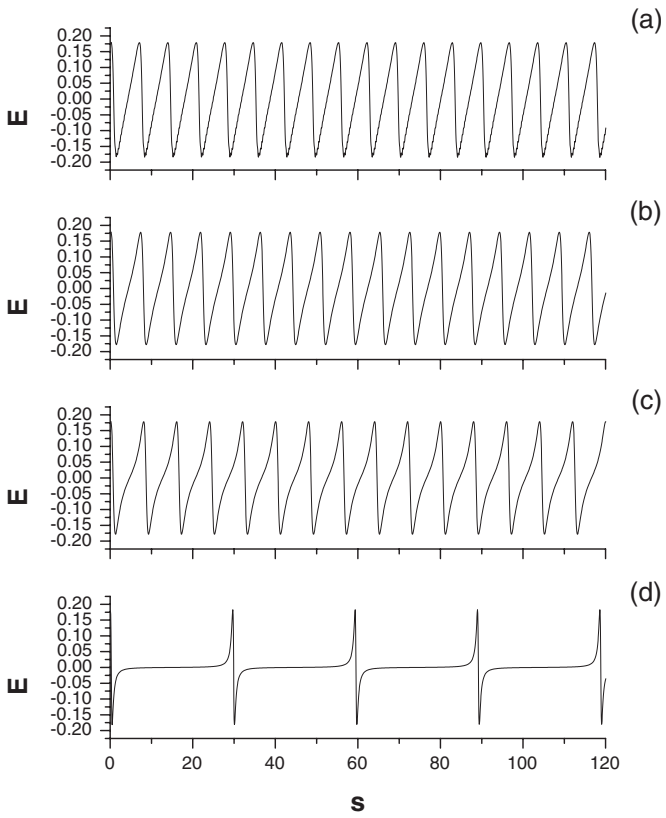

FIG. 3. The normalized parallel electric field for $E_0=0.175$ and $N_{i0}=1.0$ (a), 0.75 (b), 0.55 (c), and 0.15 (d). The other parameters are the same as in Fig. 1.

conditions have been calculated self-consistently. The results, which include the effect of the additional parameter R on the electric field structures, are discussed next.

A. Effect of the amplitude E_0 of the driving electric field

In Figs. 1(a)–1(d), the driver strength E_0 is varied for fixed value of Mach number $M=1.25$. In these figures, other fixed parameters are $\theta=2°$, $\delta=0.0$, $N_{i0}=0.75$, $R=10$, and $\alpha=0.1$. For small values of E_0, the parallel electric field shows sinusoidal behavior with a period of about $1.0\tau_{ci}$ where $\tau_{ci}=2\pi/\Omega_i$ is the ion cyclotron period. We thus identify this as being the ion cyclotron mode. This is expected as for $\alpha=0.1$, the linear IA mode is heavily damped. As E_0 increases, we have a transition to the IA mode with increasing nonlinearity which results in highly spiky structures, as in Fig. 1(d), with a period of about $3.5\tau_{ci}$. In this case the IA and ion cyclotron modes are strongly coupled through the convective terms appearing in Eqs. (4)–(6) and the IA mode appears to be nonlinearly driven by this interaction.

This behavior of the electric field with increasing E_0 is similar to that of Reddy *et al.*[42] with a slight increase in the frequencies for corresponding parameters in both studies. This effect is more significantly in the case of the nonlinear structures (i.e., for larger E_0). For $E_0=0.8$, the period of the spiky electric field of Reddy *et al.*[43] was found to be $4.0\tau_{ci}$ compared to $3.5\tau_{ci}$ in our case for the same parameters. The value of this period ($3.5\tau_{ci}$) is consistent with the measurements for $E_{\parallel}$ observed by the FAST satellite in Fig. 6 of Ergun *et al.*[6]

In Fig. 2, frequency of the spiky electric field structures is plotted against driver field E_0 for the parameters of Fig. 1. It clearly shows that the frequency of the structure decreases with the amplitude of the driver field. To start with, it is the ion cyclotron waves which are driven for low values of driver field and as driver field increases IA waves are driven and hence the decrease in frequency.

B. Effect of the oxygen ion beam density

The effect on the parallel electric field structures due to a variation in the oxygen ion beam density is shown in Figs. 3(a)–3(d). The period of oscillations increases with decreasing N_{i0} with transition from the ion cyclotron sawtooth type mode [Figs. 3(a)–3(c)] to the IA highly spiky type mode [Fig. 3(d)]. The other parameters in these figures are the same as in Fig. 1 with $E_0=0.175$. The periods vary from $1.16\tau_{ci}$ for $N_{i0}=1.0$ to $4.6\tau_{ci}$ for $N_{i0}=0.15$. This means that as the oxygen ion density decreases, we have lower frequency waves (larger periods) with increased nonlinearity. The waveform is highly spiky for $N_{i0}=0.15$ and sawtooth for larger values of the oxygen ion density. Thus, the spiky IA mode is dominant for a low initial density of the oxygen ions. For identical parameters corresponding to the quasineutral case, the period of the highly spiky waveforms (for $N_{i0}=0.15$), the period was found to be $4\tau_{ci}$ compared to $4.6\tau_{ci}$ in our case. Hence, the inclusion of the Poisson equation increases the period of the spiky waveforms in the presence of a low oxygen ion beam density. There is no significant difference in the sawtooth type oscillations between the inclusion of charge separation effects and that of quasineutrality case.[43]

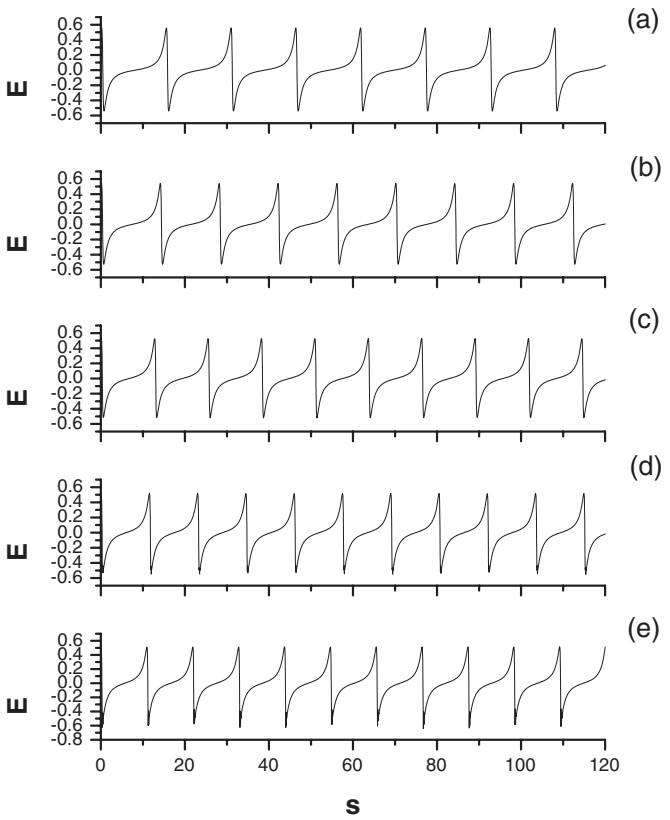

FIG. 4. Numerical solution of the normalized parallel electric field for E_0=0.5 and δ=−0.2 (a), −0.1 (b), 0.0 (c), 0.1 (d), and 0.2 (e). The other parameters are the same as in Fig. 1.

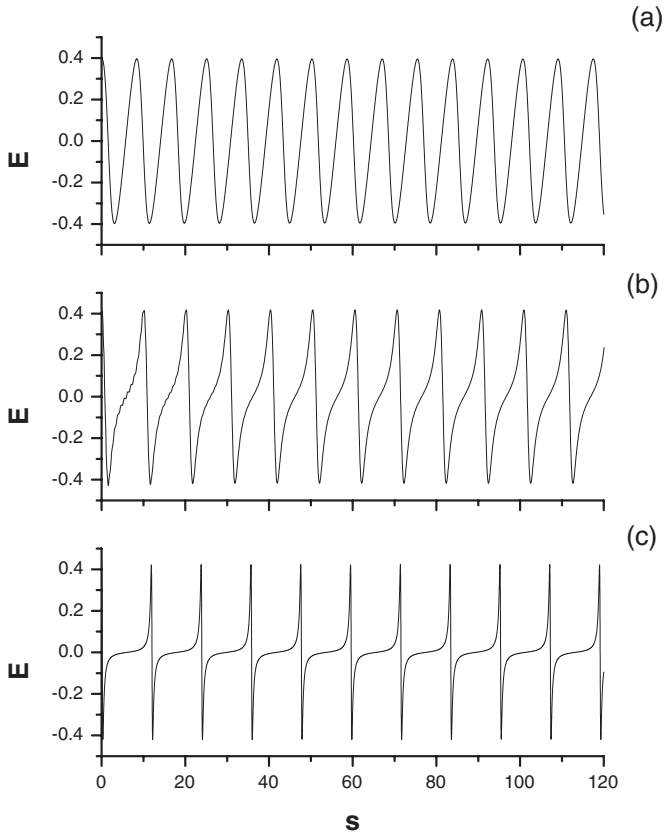

FIG. 5. Numerical solution of the normalized parallel electric field for E_0=0.4 and M=0.1 (a), 1.05 (b), and 4.5 (c). The other parameters are the same as in Fig. 1.

C. Effect of the oxygen ion drift

Next, we investigate the effect of the oxygen drift velocity on the electric field, as seen in Figs. 4(a)–4(e), with E_0=0.5 and other parameters fixed, as in Fig. 1. From these figures, it is seen that oxygen ion flow antiparallel to B_0 (δ negative) results in higher period waves and as the flow is adjusted to be parallel to B_0 (δ positive) the period decreases. All the structures were found to be of the spiky type, for the selected parameters. The period of the waves vary from $2.5\tau_{ci}$, for δ=−0.2, to $1.7\tau_{ci}$, for δ=0.2, and can be interpreted as the IA mode. The behavior of the period with the oxygen ion drift is the same as that of Moolla *et al.*[39] for the high-frequency wave studies which indicates that if the oxygen ion beam is accelerated in bursts this will produce spiky nonlinear electric field structures of different periodicity. The behavior of the electric field structures with the oxygen ion drift follows a similar pattern to that of Reddy *et al.*[43]

D. Effect of Mach number

Figures 5(a)–5(c) show the effect of the Mach number on the parallel electric field. For fixed parameters as in Fig. 1, with E_0=0.4, we vary M from 0.1 [Fig. 5(a)] to 4.5 [Fig. 5(c)]. An increase in the Mach number results in increased nonlinearity for fixed E_0 with steeper waves. Consequently, the period of the waves increases from $1.44\tau_{ci}$, for M=0.1, to $1.85\tau_{ci}$, for M=4.5. The spiky waveforms exist for $M>1$. The effect of charge separation results in an increase in the frequency of the waves, as compared to the case of Reddy *et al.*[43] for the quasineutral study.

E. Effect of propagation angle

Figures 6 and 7 display the variation in the propagation angle θ on the sawtooth and spiky electric fields, respectively. In Fig. 6, as θ increases from 2° [almost parallel propagation; Fig. 6(a)] to 85° [almost perpendicular propagation; Fig. 6(d)] the period of the oscillations decreases and all waveforms are of the sawtooth type. For small propagation angles, the IA mode is dominant, with a transition to the higher frequency ion cyclotron mode for θ=85°. The period of the waves decrease from $1.19\tau_{ci}$ to $0.83\tau_{ci}$ for θ=2° to θ=85°. The charge separation effects lead to a slight increase in the frequency of oscillation, as compared to the fully charge neutral case, for which the period were $1.28\tau_{ci}$, for θ=2°, to $0.99\tau_{ci}$, for θ=85°. In Fig. 7, we investigate the effect of the propagation angle on the spiky waveforms, using a stronger driving electric field E_0=0.8. It is seen that as the propagation angle increases, the period of the waves decrease, as was the case with the sawtooth oscillations. The periods vary from $3.4\tau_{ci}$, for θ=2°, to $2.9\tau_{ci}$, for θ=85°, with the mode remaining in the IA regime.

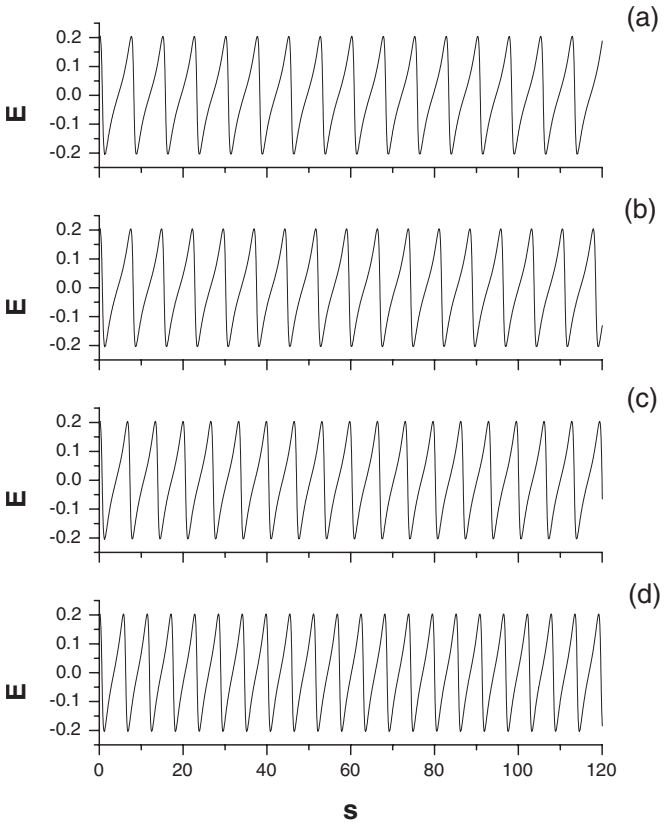

FIG. 6. Numerical solution of the normalized parallel electric field for $E_0=0.2$ and $\theta=2°$ (a), 15° (b), 40° (c), and 85° (d). The other parameters are the same as in Fig. 1.

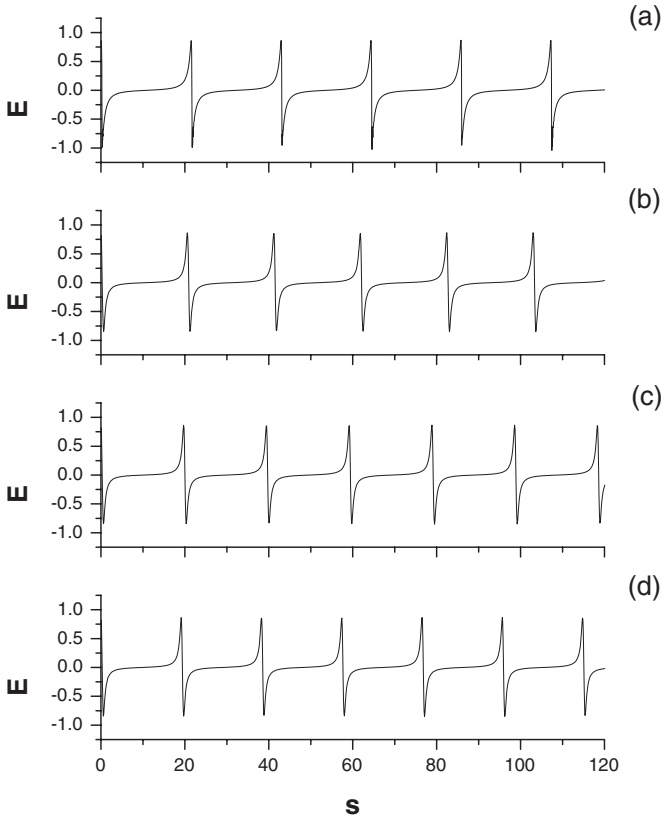

FIG. 7. Numerical solution of the normalized electric field for $E_0=0.8$ and $\theta=2°$ (a), 15° (b), 40° (c), and 85° (d). The other parameters are the same as in Fig. 1.

F. Effect of electron temperature

Figure 8 illustrates the effect of the electron-proton temperature ratio T_e/T_p on the parallel electric field. For $E_0=0.175$, with other parameters fixed as in Fig. 1, T_e/T_p is increased from 0.1 [Fig. 8(a)] to 3.0 [Fig. 8(d)]. An increase in this ratio results in waveforms with decreasing frequency and increased nonlinearity. The period of the waves increases from $1.15\tau_{ci}$ to $1.54\tau_{ci}$ as T_e/T_p increases from 0.1 to 3.0. For lower ratios, the waveforms are of the sawtooth type and the ion cyclotron mode exists. For larger ratios, the waveforms become more spiky and the period increases thus we have a transition to the IA mode. This change over from the ion cyclotron mode to the IA mode can be explained in terms of the linear properties of the modes as the driver field is small. For small values of $T_e/T_p<1.0$, the IA mode is heavily damped and only the ion cyclotron mode is excited. For $T_e/T_p>1.0$ and increasing, the linear damping is reduced and this mode can exist linearly. Then, even the low values of the driver field E_0 can lead to strong coupling between the IA and ion cyclotron modes. Further, the nonlinearity of the driven IA mode is enhanced as the thermal energy of the electron increases relative to protons. A similar behavior was observed by Reddy *et al.*[43]

G. Effect of the ion plasma to ion cyclotron frequency ratio *R*

As mentioned earlier, the use of the Poisson equation to allow for charge separation introduces an additional plasma parameter $R=\omega_{pi}/\Omega_i$, i.e., the ratio of the ion plasma frequency to the ion gyrofrequency. Figure 9 illustrates the effect of varying R on the electric field structures. It is seen that for extremely low values of R, the amplitude fluctuates showing evidence of some form of modulation. This effect disappears for much larger R values and the amplitude becomes constant. It is noted from Eq. (12) that for large values of R (a weakly magnetized plasma), the term on the right hand side of (12) becomes very large. In such situations the term on the left hand side of (12) can be neglected. This limit would then correspond to the case of quasineutrality as discussed by Reddy *et al.*[43] Consequently our findings in the limit of a strongly magnetized plasma (low R values) represents an extension of their work. In Fig. 9, for $E_0=0.5$, with the other parameters fixed as in Fig. 1, R is increased from 1.0 [Fig. 9(a)] to 50.0 [Fig. 9(d)]. In both instances, the waveforms were found to be highly spiky. The nonlinear structures do not exist for R greater than 50 and become unstructured (numerical noiselike) for $R<1$.

IV. CONCLUSION

In this paper, we have used a three component plasma model consisting of Boltzmann protons and electrons and a cold oxygen beam to study structures arising from a coupling of two low-frequency modes, namely, the oxygen ion cyclotron and the oxygen IA mode. We have extended the work of Reddy *et al.*[43] by including the Poisson equation (their studies were restricted to the quasineutrality condition). We have shown that the structures vary from sinusoidal to sawtooth to

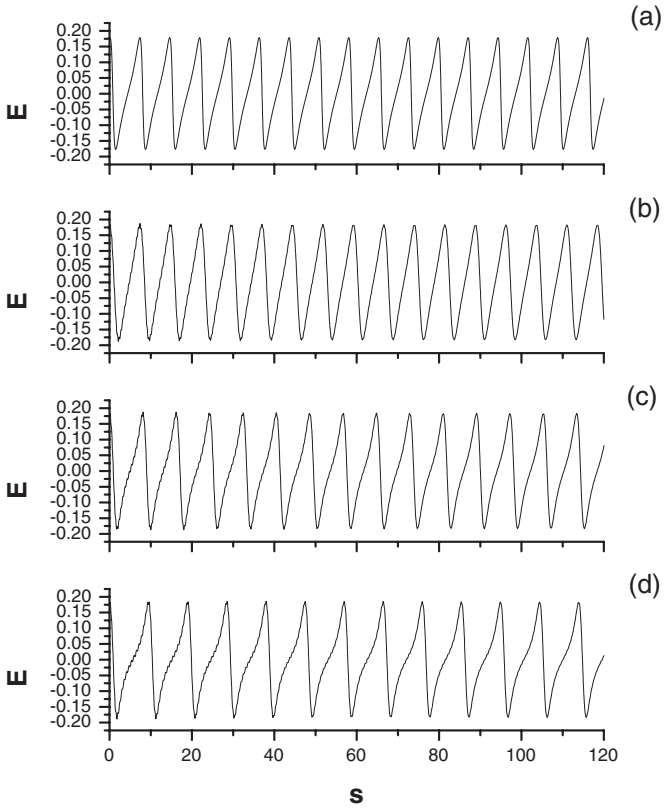

FIG. 8. Numerical solution of the normalized parallel electric field for $E_0=0.175$ and $T_e/T_p=0.1$ (a), 0.5 (b), 1.5 (c), and 3.0 (d). The other parameters are the same as in Fig. 1.

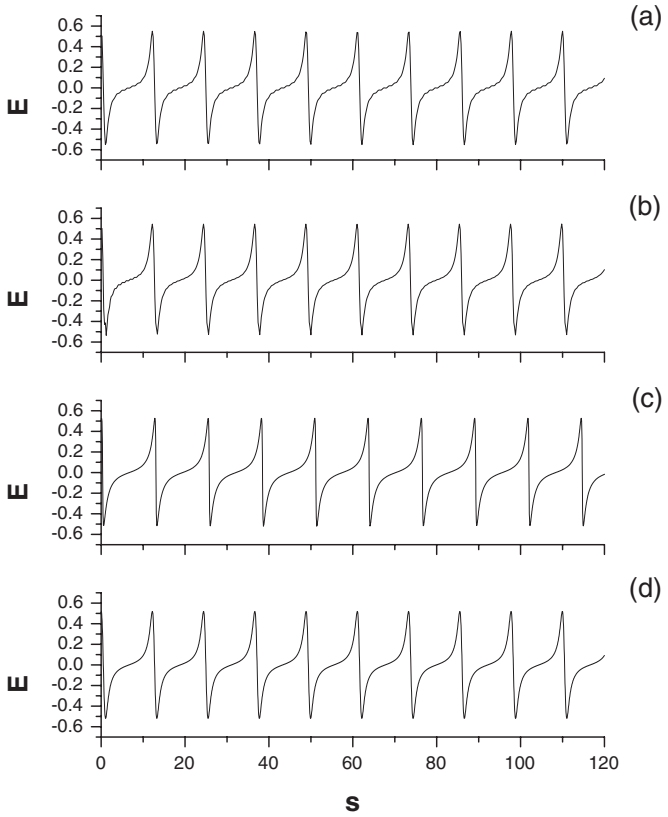

FIG. 9. Numerical solution of the normalized parallel electric field for $E_0=0.5$ and $R=1.0$ (a), 5 (b), 10 (c), and 50 (d). The other parameters are the same as in Fig. 1.

highly spiky, depending on parameter selections. The inclusion of the charge separation effect served to change the periods of the waveforms, especially for the highly spiky structures. Our studies were conducted numerically since the inclusion of the charge separation effect necessitates an explicit inclusion of the Poisson equation. This introduces a numerical complexity and the system cannot be reduced into a single nonlinear equation as was performed by Reddy *et al.*[43] The nonlinear structures are found to arise from a coupling of the IA and ion cyclotron modes, as found by Reddy *et al.*[43] We have found that larger initial driving amplitudes result in more spiky structures with a reduction in the wave frequency. We identify these as the spiky IA mode. The oxygen ion beam density also played a crucial role in evolution of the electric field structures. The driven IA mode only exists for low oxygen density, with higher oxygen densities giving rise to the ion cyclotron oscillations. The inclusion of the charge separation effect had the greatest influence on the spiky electric field structures for low oxygen ion beam densities, giving waves of much larger periods compared to those obtained using a fully quasineutrality model. In addition, the electron temperature was also found to play a role in defining the shape and time period of the electric field structures. For larger electron temperatures, the waves had increased periods and an increase in the spiky appearance. Larger electron temperatures resulted in the IA mode as opposed to the ion cyclotron mode for cooler electron temperatures. Further, the inclusion of charge separation effects in the analysis is found to slightly increase the oscillation frequency for any given values of Mach number, oxygen ion drift, and the propagation angle. An increase in the ratio ω_{pi}/Ω_i was found to produce constant amplitude waves with no modulation. Modulated waveforms were evident for smaller values of this ratio.

We have estimated the electric field associated with spiky electric field structures studied here for relevant auroral region parameters. The corresponding unnormalized electric field (E_{UN}) is given as

$$E_{\mathrm{UN}} = \frac{E}{M}\frac{T_e}{e\rho_i}. \tag{18}$$

For the typical auroral region parameters, namely, electron temperature, T_e varying from 10 to 100 eV and for a magnetic field of about 13 000 nT, from Eq. (18), electric field amplitude of these spiky structures is estimated to be in the range from 200 to 800 mV/m whereas the amplitude of the parallel electric field structures observed by the FAST satellite[6] is 700 mV/m. Thus, our theoretical estimates of the electric field amplitude are well within the range of observation.

ACKNOWLEDGMENTS

S.V.S. would like to thank the Physics Departments of University of Kwa-Zulu Natal, Durban and University of the Western Cape, Belville, South Africa for the warm hospitality during his visit and NRF, South Africa for financial sup-

port. G.S.L. thanks the Indian National Science Academy, New Delhi, India, for the support under the Senior Scientist scheme.

[1]D. A. Gurnett and L. A. Frank, J. Geophys. Res. **82**, 1031, doi:10.1029/JA082i007p01031 (1977).
[2]D. A. Gurnett and L. A. Frank, J. Geophys. Res. **83**, 1447, doi:10.1029/JA083iA04p01447 (1978).
[3]J. S. Pickett, J. D. Menietti, D. A. Gurnett, B. T. Tsurutani, P. Kintner, E. Klatt, and A. Balogh, Nonlinear Processes Geophys. **10**, 3 (2003).
[4]H. Matsumoto, H. Kojima, T. Miyatake, Y. Omura, M. Okada, and M. Tsutsui, Geophys. Res. Lett. **21**, 2915, doi:10.1029/94GL01284 (1994).
[5]F. S. Mozer, R. E. Ergun, M. Temerin, C. Cattell, J. Dombeck, and J. Wygant, Phys. Rev. Lett. **79**, 1281 (1997).
[6]R. E. Ergun, C. W. Carlson, J. P. McFadden, F. S. Mozer, G. T. Delroy, W. Peria, C. C. Chaston, M. Temerin, R. Elphic, R. Strangeway, R. Pfaff, C. A. Cattell, D. Klumpar, E. Shelley, W. Peterson, E. Moebius, and L. Kistler, Geophys. Res. Lett. **25**, 2025, doi:10.1029/98GL00635 (1998).
[7]S. D. Bale, P. J. Kellogg, D. E. Larson, R. P. Lin, K. Goetz, and R. P. Lepping, Geophys. Res. Lett. **25**, 2929, doi:10.1029/98GL02111 (1998).
[8]J. R. Franz, P. M. Kintner, and J. S. Pickett, Geophys. Res. Lett. **25**, 1277, doi:10.1029/98GL50870 (1998).
[9]B. T. Tsurutani, J. K. Arballo, G. S. Lakhina, C. M. Ho, B. Buti, J. S. Pickett, and D. A. Gurnett, Geophys. Res. Lett. **25**, 4117, doi:10.1029/1998GL900114 (1998).
[10]R. Bounds, R. F. Pfaff, S. F. Knowlton, F. S. Mozer, M. A. Temerin, and C. A. Kletzing, J. Geophys. Res. **104**, 28709, doi:10.1029/1999JA900284 (1999).
[11]C. A. Cattell, J. Dombeck, J. R. Wygant, M. K. Hudson, F. S. Mozer, M. A. Temerin, W. K. Peterson, C. A. Kletzing, C. T. Russell, and R. F. Pfaff, Geophys. Res. Lett. **26**, 425, doi:10.1029/1998GL900304 (1999).
[12]M. Temerin, K. Cerny, W. Lotko, and F. S. Mozer, Phys. Rev. Lett. **48**, 1175 (1982).
[13]R. Boström, G. Gustafsson, B. Hollback, G. Holmgren, H. Koskinen, and P. Kintner, Phys. Rev. Lett. **61**, 82 (1988).
[14]H. E. J. Koskinen, R. Lundin, and B. Holback, J. Geophys. Res. **95**, 5921, doi:10.1029/JA095iA05p05921 (1990).
[15]M. K. Hudson, W. Lotko, I. Roth, and E. Witt, J. Geophys. Res. **88**, 916, doi:10.1029/JA088iA02p00916 (1983).
[16]B. Buti, Phys. Lett. A **76**, 251 (1980).
[17]R. Bharuthram and P. K. Shukla, Phys. Fluids **29**, 3214 (1986).
[18]S. Qian, W. Lotko, and M. K. Hudson, Phys. Fluids **31**, 2190 (1988).
[19]R. V. Reddy and G. S. Lakhina, Planet. Space Sci. **39**, 1343 (1991).
[20]R. V. Reddy, G. S. Lakhina, and F. Verheest, Planet. Space Sci. **40**, 1055 (1992).
[21]M. Berthomier, R. Pottelette, and M. Malingre, J. Geophys. Res. **103**, 4261, doi:10.1029/97JA00338 (1998).
[22]G. S. Lakhina, A. P. Kakad, S. V. Singh, and F. Verheest, Phys. Plasmas **15**, 062903 (2008).
[23]G. S. Lakhina, S. V. Singh, A. P. Kakad, F. Verheest, and R. Bharuthram, Nonlinear Processes Geophys. **15**, 903 (2008).
[24]J. M. Kindel and C. F. Kennel, J. Geophys. Res. **76**, 3055, doi:10.1029/JA076i013p03055 (1971).
[25]M. C. Kelley, E. A. Bering, and F. S. Mozer, Phys. Fluids **18**, 1590 (1975).
[26]F. S. Mozer, C. W. Carlson, M. K. Hudson, R. B. Torbert, B. Parady, J. Yatteau, and M. C. Kelley, Phys. Rev. Lett. **38**, 292 (1977).
[27]M. André, H. Koskinen, G. Gustafsson, and R. Lundin, Geophys. Res. Lett. **14**, 463, doi:10.1029/GL014i004p00463 (1987).
[28]C. A. Cattell, R. Bergmann, K. Sigsbee, C. Carlson, C. Chaston, R. Ergun, J. McFadden, F. S. Mozer, M. Temerin, R. Strangeway, R. Elphic, L. Kistler, E. Moebius, L. Tang, D. Klumper, and R. Pfaff, Geophys. Res. Lett. **25**, 2053, doi:10.1029/98GL00834 (1998).
[29]N. Singh and W. C. Leung, J. Geophys. Res. **104**, 28,547, doi:10.1029/1999JA900341 (1999).
[30]T. Ohnuma, S. Miyake, T. Watanabe, T. Watari, and T. Sato, Phys. Rev. Lett. **30**, 535 (1973).
[31]T. Ohnuma, S. Miyake, T. Watanabe, T. Sato, and T. Watari, J. Phys. Soc. Jpn. **41**, 640 (1976).
[32]M. Temerin, M. Woldorff, and F. S. Mozer, Phys. Rev. Lett. **43**, 1941 (1979).
[33]L. C. Lee and J. R. Kan, Phys. Fluids **24**, 430 (1981).
[34]R. V. Reddy, G. S. Lakhina, N. Singh, and R. Bharuthram, Nonlinear Processes Geophys. **9**, 25 (2002).
[35]R. Bharuthram, R. V. Reddy, G. S. Lakhina, and N. Singh, Phys. Scr., T **98**, 137 (2002).
[36]G. Ganguli, V. Slinker, V. Gavrishchaka, and W. Scales, Phys. Plasmas **9**, 2321 (2002).
[37]G. S. Lakhina, J. Geophys. Res. **92**, 12161, doi:10.1029/JA092iA11p12161 (1987).
[38]S.-H. Kim, R. L. Merlino, and G. I. Ganguli, Phys. Plasmas **13**, 012901 (2006).
[39]S. Moolla, R. Bharuthram, S. V. Singh, and G. S. Lakhina, J. Phys. **61**, 1 (2003).
[40]S. Moolla, R. Bharuthram, S. V. Singh, G. S. Lakhina, and R. V. Reddy, J. Geophys. Res. **112**, A07214, doi:10.1029/2006JA011947 (2007).
[41]H. Kojima, H. Matsumoto, T. Miyatake, I. Nagano, A. Fujita, L. A. Frank, T. Mukai, W. R. Paterson, Y. Saito, and S. Machida, Geophys. Res. Lett. **21**, 2919, doi:10.1029/94GL02111 (1994).
[42]R. V. Reddy, S. V. Singh, R. Bharuthram, and G. S. Lakhina, Proceedings of 7th International School/Symposium For Space Simulations (ISSS-7), 26–31 March 2005 (unpublished) p. 353.
[43]R. V. Reddy, S. V. Singh, R. Bharuthram, and G. S. Lakhina, Earth Planets Space **58**, 1227 (2006).
[44]W. H. Press, S. A. Teukolsky, W. T. Vetterling, and B. P. Flannery, *Numerical Recipes in Fortran 90, The Art of Parallel Scientific Computing*, 2nd Ed. (Cambridge University Press, New York, 1996).